Polyethylene glycol (PEG)-associated immune responses triggered by clinically relevant lipid nanoparticles in rats

Haiyang Wang[1,2†], Yisha Wang[1,2†], Changzheng Yuan[3†], Xiao Xu[4], Wenbin Zhou[1,2], Yuhui Huang[3], Huan Lu[1,2], Yue Zheng[1,2], Gan Luo[1,2], Jia Shang[4], Meihua Sui[1,2*]

[1]*School of Basic Medical Sciences and Women's Hospital, Zhejiang University School of Medicine, Hangzhou, China*

[2]*Cancer Center, Zhejiang University, Hangzhou, China.*

[3]*School of Public Health, Zhejiang University School of Medicine, Hangzhou, China.*

[4]*Zhejiang University School of Medicine, Hangzhou, 310006, China*

†Equal contribution

[*]Corresponding author

Meihua Sui, M.D., Ph.D. **E-mail:** suim@zju.edu.cn

Abstract

With the large-scale vaccination of lipid nanoparticles (LNP)-based COVID-19 mRNA vaccines, elucidating the potential polyethylene glycol (PEG)-associated immune responses triggered by clinically relevant LNP has become imminent. However, inconsistent findings were observed across very limited population-based studies. Herein we initiated a study using LNP carrier of Comirnaty® as a representative, and simulated real-world clinical practice covering a series of time points and various doses correlated with approved LNP-delivered drugs in a rat model. We demonstrated the time- and dose-dependency of LNP-induced anti-PEG antibodies in rats. As a thymus-independent antigen, LNP unexpectedly induced isotype switch and immune memory, leading to rapid enhancement and longer lasting time of anti-PEG IgM and IgG upon re-injection in rats. Importantly, initial LNP injection accelerated the blood clearance of subsequent dosing in rats. These findings refine our understandings on LNP and possibly other PEG derivatives, and may promote optimization of related premarket guidelines and clinical protocols.

Lipid nanoparticles (LNP) composed of ionizable cationic lipid, cholesterol, 1,2-distearoyl-sn-glycero-3-phosphocholine (DSPC) and polyethylene glycol (PEG)-conjugated lipid, have attracted great attention due to unique advantages such as simple formulation, good biocompatibility and large payload[1]. Currently three LNP-delivered drugs have been marketed, including Patisiran (Onpattro®), mRNA vaccines BNT162b2 (Comirnaty®) and mRNA-1273 (Spikevax®)[2]. Modification of therapeutics with PEG has shown a number of advantages in several aspects[3]. Indeed, as the first vaccine using PEG as an excipient, its PEG-conjugated lipid composition (ALC-0159) plays critical roles in improving the stability and blood circulation of LNP, leading to the overwhelming success of Comirnaty®[4]. Although free PEG is poorly immunogenic, it has been recognized as a polyvalent hapten and may acquire immunogenic properties, *e.g.* inducing anti-PEG antibodies, upon conjugation with other materials such as proteins and nanocarriers[5-7]. Importantly, anti-PEG antibodies could form "antigen-antibody" complexes with newly administered PEGylated drugs, while subsequent clearance of these complexes by macrophage may lead to biodistribution/pharmacokinetic changes and reduced efficacy of PEGylated drugs[5,6]. Moreover, "antigen-antibody" complexes may induce severe side effects including hypersensitivity reactions, although the underlying mechanisms have not been fully clarified[6,8]. Interestingly, a proportion of individuals who never received PEGylated drugs have anti-PEG antibodies possibly due to environmental exposure[9,10].

With the large-scale vaccination of mRNA vaccines, elucidating the potential PEG-associated immune responses triggered by clinically relevant LNP has become urgent[11]. However, there are only five related literatures, all of which are recent clinical observations[12-16]. It is noteworthy that several limitations are existed in these studies, *e.g.* small population size[13, 15], large person-to-person variability of pre-existing anti-PEG antibodies[13, 14], age- and gender-related influences[12-14, 16], unavoidable exposure to PEG-containing substances other than LNP[12-16], deviation of sampling time points[12-16], and mixed use of different LNP-delivered drugs[14]. Currently, there is no consistent conclusion regarding any characteristic of initial and/or repeated injection of mRNA vaccines in inducing PEG-specific antibodies. Moreover, the amount of $mPEG_{2000}$ contained in each injection varies significantly among three approved LNP-delivered drugs[17-19].

56 For example, $mPEG_{2000}$ contained in each Onpattro® injection is as high as 262 times of Comirnaty®[17],
57 raising our concern on the potential impact of $mPEG_{2000}$ exposure amount on induction of PEG-associated
58 immune responses. Furthermore, as the first two vaccines using LNP as carriers, the pharmacokinetics of
59 Comirnaty® and Spikevax® might differ from previously approved intramuscular vaccines, considering that
60 the *in vivo* procedures of mRNA vaccines are mainly determined by their LNP carriers[18]. However,
61 pharmacokinetic data is not available for either Comirnaty® or Spikevax®, as these data are not regularly
62 required by WHO for market approval of intramuscular vaccines[20].

63 To clarify the cause-and-effect relationship of clinically relevant LNP in inducing PEG-associated
64 immune responses, we synthesized the LNP of Comirnaty® (most widely used clinically relevant LNP) as a
65 representative. A Wistar rat model with excellent quality control was established to eliminate undesired
66 interferences existed in previous studies. Through simulating the clinical practice of Comirnaty®, including
67 two intramuscular injections with a 21-day interval, and delicately designing clinically relevant doses
68 covering the whole range of $mPEG_{2000}$ amount contained in a single injection of approved LNP-delivered
69 drugs, the PEG-associated immune responses triggered by LNP including potential impact on
70 pharmacokinetic changes were carefully investigated.

71

72 **Results**

73 **Synthesis and physiochemical characterization of PEGylated LNP, DiR-LNP and DiR-LU@LNP**

74 LNP, DiR-LNP (LNP labeled with DiR) and DiR-LU@LNP (LNP loaded with firefly luciferase mRNA
75 and labeled with DiR) were prepared by mixing the ethanol phase containing ALC-0315, DSPC, cholesterol
76 and ALC-0159 (with or without DiR) and the aqueous phase containing citrate buffer (with or without firefly
77 luciferase mRNA) through a microfluidic mixing device (**Fig. 1a-1c**). When examined with Cryo-TEM,
78 LNP and DiR-LNP were characterized as hollow spheres, while DiR-LU@LNP exhibited a typical electron-
79 dense core structure containing mRNA (**Fig. 1c**). Further characterization with DLS showed that the Z-
80 average/PDI/Zeta potential of LNP, DiR-LNP and DiR-LU@LNP were 110.400 ± 3.466 nm/0.203 ±

0.012/16.733 ± 0.451 mV, 113.067 ± 2.139 nm/0.183 ± 0.013/7.257 ± 0.168 mV and 101.367 ± 2.593 nm/0.197 ± 0.015/-5.943 ± 0.129 mV, respectively (**Fig. 1d and 1e**; **Supplementary Table 2**). These data demonstrate that three LNP formulations have optimal particle diameter, highly monodisperse particle-size distribution and weak surface charge. Additional evaluation in the presence of 10% rat serum mimicking blood circulation showed that LNP, DiR-LNP and DiR-LU@LNP have relatively stable particle sizes and stay monodisperse (**Supplementary Fig. 1a-1c; Supplementary Figs. 2-4**). Moreover, standard curves of phospholipid (DSPC) contained in three LNP formulations were respectively drawn, as the phospholipid component is commonly used for quantifying the whole LNP[21,22]. Subsequently, clinically relevant doses of LNP including low dose (L-LNP, 0.009 mg phospholipids/kg), middle dose (M-LNP, 0.342 mg phospholipids/kg) and high dose (H-LNP, 2.358 mg phospholipids/kg) were calculated based on the corresponding equations (**Supplementary Fig. 1d-f**; see **Methods**).

Time- and dose-dependent induction of anti-PEG IgM by PEGylated LNP

After intramuscular injection of LNP at above-mentioned three doses on Day 0 and Day 21, rat serum samples were respectively collected at 12 designated time points between Day 0 and Day 49, and examined for the presence and level of anti-PEG IgM (**Fig. 2a**). Our data showed that serum anti-PEG IgM was initially detected in L-LNP group on Day 3. Although anti-PEG IgM was undetectable until Day 5 in M-LNP and H-LNP groups, both doses induced significantly higher levels of anti-PEG IgM than that induced by L-LNP. Moreover, L-LNP induced anti-PEG IgM only detectable on Day 3 and Day 5 during the first injection cycle (Day 0~21), while M-LNP and H-LNP induced more persistent and higher levels of anti-PEG IgM detectable throughout Day 5~21, suggesting a time- and dose-dependent induction of anti-PEG IgM after an initial injection of LNP. Impressively, anti-PEG IgM was detected at more time points for all three doses after repeated injection compared with that during the first injection cycle. Particularly, M-LNP and H-LNP constantly induced anti-PEG IgM throughout the whole second injection cycle and extension period (Day 21~49). Meanwhile, anti-PEG IgM levels induced by three doses exhibited a consistent ranking (H-LNP >

106 M-LNP > L-LNP) at nearly all detectable time points (**Fig. 2b**). In addition, the intra-assay
107 precision/Coefficient of Variation (CV%) of anti-PEG IgM standards and serum samples were 3.884 ± 3.046%
108 and 5.237 ± 6.192%, respectively (**Fig. 2c**), and the inter-assay precision/Coefficient of Variation (CV%) of
109 anti-PEG IgM standards and goodness of fit/coefficient of determination (R^2) of the standard curve were
110 20.983 ± 15.511% and 0.992 ± 0.004, respectively (**Fig. 2c**; **Supplementary Fig. 5**). These data demonstrate
111 the good quality control of ELISA (see **Methods** for acceptance criteria[23,24]). Overall, these data provided
112 strong evidence for the dose- and time-dependent induction of anti-PEG IgM.

113 Additionally, anti-PEG IgM production exhibited different time-course profiles across different doses
114 (**Fig. 2d**; all $P < 0.05$ in profile analysis). Further linear mixed model (LMM) analysis was conducted to
115 evaluate changes over time and differences across groups regarding anti-PEG IgM production
116 (**Supplementary Table 3**). Our data showed that β for "Group", which represents mean differences on
117 antibody level among various groups at all time points, exhibited statistical significance between Control *vs*
118 M-LNP, Control *vs* H-LNP, and L-LNP *vs* M-LNP, respectively. Significant differences were also detected
119 with β for "Time" and "Time^2", both of which representing the change rate in antibody level over time.
120 Regarding β for "Group*Time" representing mean differences in the change rate in antibody level over time
121 among various groups, we found that compared with the Control group, M-LNP and H-LNP groups showed
122 faster rate of anti-PEG IgM production, with H-LNP group exhibited the fastest rate among all the groups,
123 which further demonstrated the above-mentioned dose- and time- dependency. Moreover, consistent with
124 the longer lasting period and higher level of anti-PEG IgM induced by repeated LNP injection, LMM
125 analysis revealed the significant difference on antibody level between two separate injections (β for "Second
126 Injection": $P < 0.0001$ *vs* First Injection).

127

128 **Time- and dose-dependent induction of anti-PEG IgG by PEGylated LNP**

129 Serum samples collected at above-mentioned time points were further examined for anti-PEG IgG (**Fig.**
130 **3a**). Interestingly, different from anti-PEG IgM production, no anti-PEG IgG was detected throughout the

131 first injection cycle in all experimental groups. These data suggest that an initial single injection of LNP, at
132 a broad range of doses, could not induce anti-PEG IgG in rats. However, although anti-PEG IgG was still
133 undetectable after the second L-LNP injection, it was clearly induced by the repeated injection of M-LNP
134 and H-LNP, and persisted at all later time points (Day 24~49). Similar to the dose-dependency of anti-PEG
135 IgM, anti-PEG IgG levels induced by H-LNP were significantly higher than corresponding levels induced
136 by M-LNP at all detectable time points, with peak levels achieved on Day 26 for both M-LNP and H-LNP
137 groups. Moreover, the intra-assay precision/Coefficient of Variation (CV%) of anti-PEG IgG standards and
138 serum samples were 4.897 ± 5.549% and 8.546 ± 12.211%, respectively, and the inter-assay
139 precision/Coefficient of Variation (CV%) of anti-PEG IgG standards and goodness of fit/coefficient of
140 determination (R^2) were 24.896 ± 10.071% and 0.999 ± 0.001, respectively (**Fig. 3b**; **Supplementary Fig.**
141 **6**), all of which demonstrating the good quality control of ELISA (see **Methods** for acceptance criteria[23,24]).
142 As depicted in **Fig. 3c**, Control and L-LNP groups had similar time-course profile in anti-PEG IgG
143 production ($P > 0.05$ in profile analysis), whereas every other two groups exhibited different profiles (all P
144 < 0.05 in profile analysis). Further LMM analysis was conducted to evaluate the changes of anti-PEG IgG
145 over time and differences across groups (**Supplementary Table 4**). β for "Group" exhibited statistical
146 significance between M-LNP *vs* L-LNP and H-LNP *vs* L-LNP. Similar to anti-PEG IgM induction,
147 significant differences were detected with β for "Time" and "Time^2". Meanwhile, both M-LNP and H-LNP
148 groups had faster rate of anti-PEG IgG production compared with the Control group regarding β for
149 "Group*Time", with H-LNP group exhibited the fastest rate among all experimental groups. These data
150 further demonstrate dose- and time- dependent induction of anti-PEG IgG by LNP. Correspondingly, LMM
151 analysis confirmed the significant difference on anti-PEG IgG level between the two separate injections (β
152 for "Second Injection": $P < 0.0001$ *vs* First Injection).
153

154 **Enhanced production of anti-PEG antibodies by previous exposure to PEGylated LNP**

155 To quantify the potential influence of initial/previous exposure to LNP on the production of anti-PEG

156 antibodies after repeated LNP injection, increased anti-PEG IgM (▲Anti-PEG IgM (Log_{10} CONC)) and
157 increased anti-PEG IgG (▲Anti-PEG IgG (Log_{10} CONC)) were respectively calculated by subtracting
158 log10-transformed anti-PEG antibody concentration after first injection from that after the second injection
159 for all tested doses and time points (▲Day 0, 3, 5, 7, 14 and 21). Our data showed that although ▲Anti-
160 PEG IgM (Log_{10} CONC) was undetectable until ▲Day 5 in L-LNP group, significantly increased anti-PEG
161 IgM production was observed at all time points in M-LNP and H-LNP groups. Moreover, two sequential
162 injections of L-LNP induced transient ▲Anti-PEG IgM (Log_{10} CONC) detectable on ▲Day 5~14, while
163 those of M-LNP and L-LNP induced more persistent and higher level of ▲Anti-PEG IgM (Log_{10} CONC)
164 detectable throughout ▲Day 3~21 (**Fig. 4a**). Further profile analysis revealed that time-course of▲Anti-
165 PEG IgM (Log_{10} CONC) between every two groups exhibited different profiles (**Fig. 4b**; all $P < 0.05$ in
166 profile analysis). Coincidentally, LMM analysis demonstrated statistical significance on ▲Anti-PEG IgM
167 (Log_{10} CONC) changes over 6 time points (except for H-LNP *vs* M-LNP) and differences across 3 doses
168 (**Supplementary Table 5**). For instance, ▲Anti-PEG IgM (Log_{10} CONC) ranking from low to high was that
169 respectively induced by L-LNP, M-LNP and H-LNP at all detectable time points regarding β for "Group",
170 demonstrating the dose dependency of ▲Anti-PEG IgM (Log_{10} CONC). Additionally, change rate in ▲Anti-
171 PEG IgM (Log_{10} CONC) exhibited significant differences over 6 time points, with $P < 0.0001$ for both "Time"
172 and "$Time^2$". Regarding β for "Group*Time", M-LNP and H-LNP groups had faster change rate in ▲Anti-
173 PEG IgM (Log_{10} CONC) than L-LNP group. These data have provided additional evidence for dose- and
174 time- dependency of ▲Anti-PEG IgM (Log_{10} CONC) induced by two sequential injections of LNP.

175 As anti-PEG IgG was absent throughout the first injection cycle and in all L-LNP-treated groups,
176 ▲Anti-PEG IgG (Log_{10} CONC) was detected on ▲Day 3~21 in M-LNP and H-LNP groups（**Fig. 4c**). Our
177 data showed that the time-course profiles of ▲Anti-PEG IgG (Log_{10} CONC) exhibited significant difference
178 among all other experimental groups (all $P < 0.05$ in profile analysis), except that no difference between
179 Control and L-LNP groups was found ($P > 0.05$ in profile analysis). Corresponding LMM analysis further
180 confirmed these findings (**Supplementary Table 6**), as statistical significances were obtained for ▲Anti-

181 PEG IgG (Log_{10} CONC) among Control/L-LNP, M-LNP and H-LNP groups regarding β for "Group".
182 Together with the significant differences for "Time" and "$Time^2$" on change rate over 6 time points, our data
183 clearly demonstrated that similar to anti-PEG IgM, an initial/previous injection of LNP dose- and time-
184 dependently boosted the generation of anti-PEG IgG after the repeated injection.
185

186 **Dose-dependent biodistribution of PEGylated LNP administered at clinically relevant doses**

187 By using a fluorescence and bioluminescence double-labeling strategy, the biodistribution of LNP was
188 determined in rats treated with DiR-LU@LNP simulating clinical practice (**Fig. 5a**). Consistent with the
189 preclinical biodistribution data published in Assessment Report of Comirnaty® issued by the European
190 Medicines Agency, weak bioluminescence signal of luciferase was detected in muscle at injection site and
191 liver (**Supplementary Fig. 7**), demonstrating that DiR-LU@LNP drained into the liver and delivered active
192 luciferase mRNA. As DiR fluorescence exhibited significantly higher sensitivity than luciferase
193 bioluminescence (**Fig. 5b**; **Supplementary Fig. 7**), LNP biodistribution was further analyzed based on DiR
194 fluorescence. Our data showed that 6 hours after both the first and second injections, DiR fluorescence was
195 only detectable in muscle at the injection site in L-LNP group. Upon increase of LNP dose, the fluorescent
196 signal was significantly enhanced and detected in more organs/tissues (muscle at the injection site, liver and
197 lung in M-LNP group; muscle at the injection site, liver, lung, spleen and draining lymph node in H-LNP
198 group). Further analysis indicated that the total radiant efficiency from liver, lung, spleen and heart exhibited
199 statistical significance between Control *vs* M-LNP, Control *vs* H-LNP, L-LNP *vs* M-LNP, L-LNP *vs* H-LNP,
200 and M-LNP *vs* H-LNP after both the first and second injections. These findings demonstrate a dose-
201 dependent biodistribution of LNP, with preferential accumulation in reticuloendothelial system after entering
202 the blood circulation *via* intramuscular injection (**Fig. 5b and 5c**).
203

204 **Accelerated blood clearance induced by repeated injection of PEGylated LNP administered at**
205 **clinically relevant dose**

206 To explore whether previous exposure would alter the pharmacokinetic of repeatedly or newly injected
207 LNP, rats were injected with DiR-LNP at above-mentioned doses and schedule, followed by collection of
208 serum samples at 8 time points after each injection and measurement of DiR fluorescence (**Fig. 6a**). Our data
209 indicate that LNP-associated DiR fluorescence was undetectable in L-LNP group at all time points after both
210 injections, suggesting a low level of LNP in blood circulation after administration of low dose DiR-LNP. As
211 expected, DiR fluorescence was significantly increased in serums isolated from M-LNP (at 6 and 10 hours)
212 and H-LNP (at 7 sequential time points between 30 minutes and 48 hours) groups after the initial injection
213 of DiR-LNP. However, compared with the first injection, DiR fluorescence was detected at less time points
214 in M-LNP (only 6 hours) and H-LNP (4 sequential time points between 6 and 48 hours) groups after the
215 second injection of DiR-LNP, indicating faster blood clearance and reduced serum level of LNP upon
216 repeated administrations (**Fig. 6b**). Indeed, as depicted in **Fig. 6c and 6d**, DiR fluorescence was significantly
217 decreased at 30 minutes, 1 hour and 48 hours after repeated injection of high dose DiR-LNP compared with
218 that after the initial injection. These data demonstrate for the first time an accelerated blood clearance (ABC)
219 phenomenon of clinically relevant LNP.
220

221 **Discussion**

222 PEG-related immune responses induced by clinically relevant LNP may directly affect the clinical
223 outcome of LNP-delivered drugs[11]. However, it is practically difficult to clarify these issues simply with
224 clinical investigations. One major reason is the significant variability of pre-existing PEG-specific antibodies,
225 making it extremely hard to identify anti-PEG antibodies specifically induced by LNP (**Supplementary**
226 **Discussion**). Another concern is additional exposure to PEG derivatives other than LNP possibly existed
227 during clinical observation period. In agreement with this, Ju *et al* reported that unvaccinated control donors
228 had increased level of anti-PEG IgG and/or anti-PEG IgM in their clinical study[13]. Together with other
229 above-mentioned influence factors existed in clinical studies such as small population size and varied
230 $mPEG_{2000}$ exposure amount, these limitations have led to inconsistent data regarding the characteristic of

231 initial and repeated exposure to LNP-delivered drugs in inducing anti-PEG antibodies (**Supplementary**
232 **Discussion**). Motivated by these challenges, we initiated the first animal study using a model LNP with the
233 largest number of recipients all over the world, and delicately simulated clinical practice for both schedule
234 and doses. Anti-PEG antibody was undetectable in all experimental groups before initial LNP injection,
235 demonstrating a "clean" background of our model system. Encouragingly, through designing a series of time
236 points and three doses (1:38:262) correlated with the amount of $mPEG_{2000}$ contained in approved LNP-
237 delivered drugs, we demonstrated for the first time that induction of anti-PEG IgM and IgG were both time-
238 and dose-dependent, which are valuable for LNP-based research and development.

239 In spite of the significant difference between mRNA vaccines from traditional vaccines, no
240 pharmacokinetic studies have been conducted for either approved mRNA vaccines or their LNP carriers[25,26].
241 Herein, we conducted the first pharmacokinetic study related with LNP-delivered vaccines or their LNP
242 carriers. Our data suggest that previous LNP injection may accelerate the blood clearance of subsequently
243 administered LNP, which has raised an important and clinically relevant issue that would warrant further
244 investigation. It is noteworthy that although Alnylam Pharmaceuticals *Inc.* reported the absence of ABC
245 phenomenon after repeated injection of Onpattro®, all patients in their study received corticosteroid
246 premedication prior to each Onpattro® injection to reduce the risk of infusion-related reactions[12]. However,
247 corticosteroid is generally considered as an immunosuppressive drug and may repress PEG-associated
248 immunological effects. To the best of our knowledge, previously there is no report investigating whether
249 intramuscularly injected PEGylated therapeutics could induce accelerated blood clearance. Our data would
250 thereby provide valuable information for revealing the pharmacokinetic characteristics of intramuscularly
251 administered PEGylated therapeutics (**Supplementary Discussion**). Together with further in-depth studies
252 using larger sample size, our findings may promote the optimization of premarket requirements and clinical
253 practice for LNP-delivered biomedical products, as well as PEGylated products administered
254 intramuscularly (**Supplementary Discussion**).

255 Similar to PEGylated liposome, LNP belongs to thymus-independent antigens (TI-Ag) as it contains no

256 proteinatious composition[5,8]. There is a traditional perception that TI-Ag could not induce isotype switch
257 from IgM to long-lasting IgG, resulting in IgM production only after TI-Ag administration, with no or very
258 low level of IgG[8]. Moreover, different from thymus-dependent antigens (TD-Ag), TI-Ag generally could not
259 induce B cell memory[27]. That is, an amplified, accelerated and affinity-matured antibody production could
260 be observed after successive exposure to TD-Ag but not TI-Ag[27]. Consistent with these theories, even six
261 repeated injections of PEGylated liposome neither enhanced anti-PEG IgM production nor effectively
262 induced anti-PEG IgG in mice[28]. Unexpectedly, we discovered that LNP not only induced isotype switch
263 and production of anti-PEG IgG, but caused B cell memory, leading to rapid enhancement and longer lasting
264 time of both anti-PEG IgM and IgG upon repeated injections (**Supplementary Fig. 8**). To our best
265 knowledge, there is no previous report on either inducing B cell memory or isotype switching from IgM to
266 IgG by any PEGylated TI-Ag (**Supplementary Discussion**). These findings refine our understandings on
267 PEGylated LNP, and possible other PEG derivatives.
268

269 **Methods**

270 **Materials**

271 Cholesterol (Cat. No. 57-88-5) and DSPC (Cat. No. 816-94-4) were purchased from Lipoid GMBH
272 (Ludwigshafen, Germany). ALC-0315 (Cat. No. 06040008600) and ALC-0159 (Cat. No. 06020112302)
273 were acquired from SINOPEG (Xiamen, China). Ferric chloride hexahydrate (Cat. No. 701122), ammonium
274 thiocyanate (Cat. No. 221988) and NH_2-PEG_{10000}-NH_2 (Cat. No. 8218815000) were obtained from Sigma-
275 Aldrich (St. Louis, MO, USA). 3-[(3-cholamidopropyl)dimethylammonio]-1-propanesulfonate (CHAPS,
276 Cat. No. ST1145), 3,3′,5,5′-tetramethylbenzidine dihydrochloride hydrate (TMB 2HCl, Cat. No. ST1708)
277 and nonfat powdered milk (Cat. No. P0216) were purchased from Beyotime Biotechnology (Shanghai,
278 China). 1,1-dioctadecyl-3,3,3,3-tetramethylindotricarbocyaine iodide (DiR, Cat. No. 100068-60-8) was
279 purchased from Shanghai Maokang Biotechnology Co., Ltd. (Shanghai, China). Maxisorp 96-well
280 microplates (Cat. No. 44-2404-21) were acquired from Nalge-Nunc International (Rochester, NY, USA). D-

281 Luciferin (Cat. No. 88293) were purchased from Thermo Fisher Scientific (Waltham, MA, USA). Firefly
282 luciferase mRNA (Cat. No. L-7702-1000) was obtained from Trilink Biotechnologies (San Diego, CA, USA).
283 Rat anti-PEG IgM (Cat. No. rAGP6-PABM-A; Clone No. rAGP6) and rat anti-PEG IgG (Cat. No. r33G-
284 PABG-A; Clone No. r33G) were acquired from Academia Sinica (Taipei, China). Peroxidase-conjugated
285 affinipure rabbit anti-rat IgM μ-chain specific (Cat. No. 312-035-020; Clone No. 312-035-020) and
286 peroxidase-conjugated affinipure donkey anti-rat IgG (H+L) (Cat. No. 712-035-150; Clone No. 712-035-
287 150) were obtained from Jackson ImmunoResearch Laboratories Inc (West Grove, PA, USA).
288

289 **Preparation of LNP, DiR-LNP and DiR-LU@LNP**

290 LNP, DiR-LNP and DiR-LU@LNP were formulated according to a previously reported protocol[29]. First,
291 the ethanol phase was prepared by dissolving ALC-0315, DSPC, cholesterol and ALC-0159 at a molar ratio
292 of 46.3: 9.4: 42.7: 1.6. Specifically, DiR was added into the ethanol phase at 0.4% mol for preparation of
293 DiR-LNP and DiR-LU@LNP. Regarding the aqueous phase, it was prepared using 20 mM citrate buffer
294 (pH4.0) for LNP and DiR-LNP formulations, with additional firefly luciferase mRNA added for DiR-
295 LU@LNP formulation. Subsequently, the ethanol phase was mixed with the aqueous phase at a flow rate
296 ratio of 1: 3 (ethanol: aqueous) through a microfluidic mixer (Precision Nanosystems Inc., Canada).
297 Afterwards, the obtained nanoparticle solutions were dialyzed against 10 × volume of PBS (pH7.4) through
298 a tangential-flow filtration (TFF) membrane with 100 kD molecular weight cut-off (Sartorius Stedim Biotech,
299 Germany) for at least 18 hours. Finally, nanoparticle solutions were concentrated using Amicon ultra-
300 centrifugal filters (EMD Millipore, Billerica, MA, USA), passed through a 0.22 μm filter and stored at 2~8 ℃
301 until use.
302

303 **Characterization of LNP, DiR-LNP and DiR-LU@LNP**

304 LNP, DiR-LNP and DiR-LU@LNP were examined for their hydrodynamic size (Z-average),
305 polydispersity index (PDI) and zeta potential with DLS (Zetasizer Nano ZS, Malvern Instruments Ltd,

306 Malvern, UK) equipped with a solid state HeNe laser (λ = 633 nm) at a scattering angle of 173°.
307 Nanoparticles were either added into PBS (pH7.4) for Z-average and PDI measurements, or added into
308 ultrapure water for determination of zeta potential. Three independent experiments were conducted, with
309 each type of LNP examined at 25 ℃ for 10 seconds (pre-equilibration for 2 minutes) and repeated at least
310 10 times in disposable cuvettes (for Z-average and PDI) or zeta cuvettes (for zeta potential). The obtained
311 data were presented as "mean ± standard deviation". To further assess their stability in serum (simulating in
312 vivo environment in this study), LNP, DiR-LNP and DiR-LU@LNP were diluted to 1:100 with PBS
313 containing 10% rat serum and then incubated at 37 ℃ for 24 hours. Subsequently, 1 mL of diluted LNP,
314 DiR-LNP and DiR-LU@LNP were respectively collected at designated time points (1 hour, 6 hours, 12 and
315 24 hours post-incubation), followed by characterization of Z-average and PDI with DLS. Three independent
316 experiments were conducted, with each type of LNP examined at 37 ℃ for 10 seconds (pre-equilibration for
317 2 minutes) and repeated at least 10 times in disposable cuvettes. The obtained data were presented as "mean
318 ± standard deviation". Furthermore, the morphological characteristics of LNP, DiR-LNP and DiR-LU@LNP
319 were observed with Cryo-TEM. In brief, 3 μL of each LNP sample was deposited onto a holey carbon grid
320 that was glow-discharged (Quantifoil R1.2/1.3) and vitrificated using a Vitrobot Mark IV System
321 (FEI/Thermo Scientific, Waltham, MA, USA). Cryo-TEM imaging was performed on a Talos F200C device
322 (FEI/Thermo Scientific, Waltham, MA, USA) equipped with a 4k × 4k Ceta camera at 200 kV accelerating
323 voltage in the Center of Cryo-Electron Microscopy, Zhejiang University.

324 In addition, the phospholipid (DSPC) concentrations of LNP, DiR-LNP and DiR-LU@LNP solutions
325 were quantified via Steward's assay for further calculation of LNP doses[30]. Briefly, ammonium
326 ferrothiocynate was prepared by dissolving 27.03 mg ferric chloride hexahydrate and 30.4 mg ammonium
327 thiocyanate in 1 mL of distilled water. 10 μL of the lipid sample was added to 990 μL of chloroform, followed
328 by addition of 1 mL of ammonium ferrothiocynate. The obtained mixture was vortexed for 60 seconds and
329 then centrifuged at 300 × g for 15 minutes at room temperature. The bottom chloroform layer was transferred
330 to a glass cuvette and the absorbance was measured at 470 nm using a Unicam UV500 Spectrophotometer

331 (Thermo electron corporation, USA). Standard curves for DSPC lipid were obtained and used for calculation
332 of the phospholipid concentrations of LNP, DiR-LNP and DiR-LU@LNP solutions. Eventually, the various
333 doses of LNP tested in the animal experiments were calculated based on the phospholipid (DSPC) exposure
334 amount per dose of related drug (see below for details).
335
336 **Determination of LNP dosing protocols**
337 According to the official drug information and clinical protocols, the $mPEG_{2000}$ exposure amount for
338 each injection of Comirnaty® in adults is 0.0406 mg[18], while that for Onpattro® is 10.6434 mg[17] (262 folds
339 of that of Comirnaty®). Different from Comirnaty® and Onpattro®, the detailed LNP composition of
340 Spikevax® including the molar lipid ratios is not included in the official drug information published in 2022[19].
341 With a postulation that PEG_{2000}-DMG is the only lipid contained in LNP of Spikevax®, we estimated that
342 the possible "maximum" $mPEG_{2000}$ exposure for each injection would be 1.542 mg (37.98 folds of that of
343 Comirnaty®) referred to the clinical protocols of Spikevax®[19](**Supplementary Methods; Supplementary**
344 **Table 1**).
345 Based on the above calculation and estimation, three $mPEG_{2000}$ dosages including 0.0406 mg/dose (low
346 dose), 1.542 mg/dose (middle dose) and 10.6434 mg/dose (high dose) were obtained. These dosages not
347 only have an appropriate gradient ratio of 1:38:262, but cover the broad range of PEG exposure amount upon
348 each injection of approved LNP-delivered drugs.
349 Next, we calculated the phospholipid (DSPC) contained in LNP of Comirnaty®, which is 0.09 mg for
350 each injection in adults[18]. According to the animal-human dose exchange algorithm: animal equivalent dose
351 = human dose × K_m ratio (6.2 for rat)[31], clinically relevant LNP doses for rats were as follows: low dose (L-
352 LNP), 0.009 mg phospolipid/kg (0.09 mg/60 kg × 6.2); middle dose (M-LNP), 0.342 mg phospholipids/kg
353 (0.009 × 38); high dose (H-LNP), 2.358 mg phospholipids/kg (0.009 × 262).
354 The clinical protocols of Comirnaty® were essentially simulated in this study. That is, LNP was
355 administrated through intramuscular injection for two separate injections, with a 21-day interval (same as

356 routine Comirnaty® vaccination).

357

358 **Animals**

359 10-12-week-old female Wistar rats were purchased from Hangzhou Medical College (Hangzhou,
360 China), and maintained in the Laboratory Animal Center of Zhejiang University under controlled
361 environmental conditions at constant temperature, humidity, and a 12-hour dark/light cycle. Rats were given
362 ad libitum access to a standard rat chow and water, and were acclimated for at least 7 days. All animal
363 experiments were approved by the Laboratory Animal Welfare and Ethnics Committee of Zhejiang
364 University and carried out in accordance with the guidelines of the committee (approval No. ZJU20210071).

365

366 **Administration of LNP simulating clinical protocols and collection of serum samples for ELISA**

367 Wistar rats were randomly divided into a Control group (n = 8) and three LNP-treated groups (n = 15).
368 At Day 0, LNP-treated groups were intramuscularly injected with 0.009 mg phospholipids/kg LNP (L-LNP
369 group), 0.342 mg phospholipids/kg LNP (M-LNP group) and 2.358 mg phospholipids/kg LNP (H-LNP
370 group), respectively, while the Control group only received PBS. At Day 21, rats in each experimental group
371 received same treatment as the initial injection. Peripheral blood samples of each rat were collected
372 successively via the retro-orbital venous plexus at Day 0, 3, 5, 7, 14, 21, 24, 26, 28, 35, 42 and 49. All blood
373 samples were centrifuged at 2000 × g for 15 minutes at 4 °C, and the serums were immediately stored at -
374 80 °C for further quantification of anti-PEG antibody. At the experimental endpoint, the animals were
375 humanely euthanized through intraperitoneal administration of 150mg/kg of sodium pentobarbital salt (Cat.
376 No. BCP07810, Biochempartner, Shanghai, China)[32].

377

378 **Quantification of anti-PEG IgM and anti-PEG IgG antibodies with ELISA**

379 Maxisorp® 96-well microplates were coated with 5 μg/well NH_2-PEG_{10000}-NH_2 in 100 μL of PBS
380 overnight at 4 °C. Subsequently, plates were gently washed with 350 μL of washing buffer (0.05% (w/v)

381 CHAPS in DPBS) for three times, followed by incubation with blocking buffer (5% (w/v) skim milk powder
382 in DPBS, 200 μL/well) at room temperature for 1.5 hours. Afterwards, plates were rinsed with washing
383 buffer for three times again. Then 100 μL of rat serum samples diluted 1: 150 with dilution buffer (2% (w/v)
384 skim milk powder in DPBS), together with seven serial dilutions of rat anti-PEG IgM standards (1.37, 4.12,
385 12.35, 37.04, 111.11, 333.33 and 1000.00 ng/mL) or rat anti-PEG IgG standards (0.05, 0.15, 0.46, 1.37, 4.12,
386 12.35 and 37.04 ng/mL), were added into anti-PEG IgM or anti-PEG IgG detection plates in duplicate and
387 further incubated for 1 hour at room temperature. After five successive washes, 50 μL of diluted peroxidase-
388 conjugated affinipure rabbit anti-rat IgM μ-chain specific and peroxidase-conjugated affinipure donkey anti-
389 rat IgG (H+L) antibodies were respectively added at 0.08 μg/mL to the corresponding plates and incubated
390 for 1 hour at room temperature. Again, unbounded antibodies were removed by five washes, followed by
391 incubation with 100 μL of TMB for 30 minutes at room temperature. Finally, HRP-TMB reaction was
392 stopped with 100 μL of 2 N H_2SO_4, and the absorbance was measured at 450 nm with a microplate reader
393 (Thermo Fisher Scientific, Waltham, MA, USA), using 570 nm as a reference wavelength. Anti-PEG IgM
394 and anti-PEG IgG standard curves in each batch of ELISA were constructed by plotting the average corrected
395 absorbance values ($OD_{450\ nm}$-$OD_{570\ nm}$) and corresponding antibody concentrations with Four Parameter
396 Logistic (4PL) curve fit using Origin 2021 software (OriginLab Corporation, Northampton, Massachusetts,
397 USA). The goodness of fit of each standard curve was measured by the coefficient of determination (R^2)[33].
398 Concentrations of anti-PEG IgG and IgM antibodies in serum samples were calculated based on
399 corresponding standard curves. In addition, intra-assay precision was evaluated by calculating the
400 Coefficient of Variation (CV% = (Standard deviation/Mean) × 100%) for all detectable standards and
401 samples in all batches of ELISA[23,24]. Inter-assay precision was determined by calculating the Coefficient of
402 Variation for serially diluted anti-PEG antibody standards among all batches of ELISA[23,24]. The acceptance
403 criteria for mean intra-assay and inter-assay Coefficient of Variation (CV%) of ELISA are < 20% and < 25%,
404 respectively[23,24].
405

406 **Biodistribution of PEGylated LNP in major organs of Wistar rats**

407 Wistar rats were randomly divided into a Control group and three DiR-LU@LNP-treated groups (n =
408 6). At Day 0, LNP-treated groups were intramuscularly injected with 0.009 mg phospholipids/kg DiR-
409 LU@LNP (L-LNP group), 0.342 mg phospholipids/kg DiR-LU@LNP (M-LNP group) and 2.358 mg
410 phospholipids/kg DiR-LU@LNP (H-LNP group), respectively, while the Control group only received PBS.
411 At Day 21, rats in each experimental group received same treatment as the initial injection. Six hours after
412 the first and second injections, three rats in each group were administered intraperitoneally with D-luciferin
413 at a dose of 150 mg/kg. Rats were sacrificed by cervical dislocation 15 minutes after D-luciferin
414 administration and immediately dissected for collection of several primary organs, including heart, liver,
415 spleen, lung, kidneys, draining lymph node and muscle at the injection site. Whole-organ/tissue imaginings
416 for DiR fluorescence (Excitation/Emission: 748 nm/780 nm) and firefly luciferase bioluminescence were
417 performed with IVIS Spectrum imaging system and analyzed with Living Image software (Caliper Life
418 Sciences, Waltham, Massachusetts, USA).

419

420 **Blood clearance of PEGylated LNP in Wistar rats**

421 Wistar rats were randomly divided into a Control group and three DiR-LNP-treated groups (n = 3). At
422 Day 0, LNP-treated groups were intramuscularly injected with 0.009 mg phospholipids/kg DiR-LNP (L-
423 LNP group), 0.342 mg phospholipids/kg DiR-LNP (M-LNP group) and 2.358 mg phospholipids/kg DiR-
424 LNP (H-LNP group), respectively, while the Control group only received PBS. At Day 21, rats in each
425 experimental group received same treatment as the initial injection. Peripheral blood samples were
426 respectively collected from the retro-orbital venous plexus at 5 minutes, 30 minutes, 1 hour, 3 hours, 6 hours,
427 10 hours, 24 and 48 hours after the first and second injections. Then blood samples were centrifuged at 2000
428 × g at 4 °C for 15 minutes, and serum samples were isolated and immediately stored in dark at -80 °C. DiR
429 fluorescence associated with LNP in serum samples was detected by fluorescent spectroscopy on a
430 Spectramax ID5 (Molecular Devices, San Jose, California, USA) at excitation/emission wavelengths of

748/780 nm. At the experimental endpoint, the animals were humanely euthanized through intraperitoneal administration of 150mg/kg of sodium pentobarbital salt (Cat. No. BCP07810, Biochempartner, Shanghai, China)[32].

Data presentation and statistical analysis

All data were presented as "mean ± standard deviation". Concentrations (ng/mL) of anti-PEG IgM and anti-PEG IgG were analyzed after $\log_{10}$ transformation, and their differences among various groups at each time point were analyzed with Mann-Whitney U test using R 4.0.5 (R Software, Boston, MA, USA), with *P* values adjusted with FDR (false discovery rate) method. Changing curves of average level of anti-PEG antibody over time for various doses were fitted by the R package called "ggalt". Profile analysis was performed to examine whether the overall trends of changing curves of average level of anti-PEG antibody over time between every two groups were equal. The analysis included two parts: parallel test and coincidence test. Only when the two changing curves of average level of anti-PEG antibody met both parallel and coincidence test ($P > 0.05$), the overall trend of two changing curves of average anti-PEG antibody level was considered as no statistical difference. According to factorial design (group × time) and repeated measures of antibody level, linear mixed models (LMM) were conducted to compare the change rates and average levels of anti-PEG antibody across groups, with all time points included. Several variables, including group (indicating mean differences in the average levels of anti-PEG antibody), time, $time^2$, number of injections, and interaction term of group and time (indicating mean differences in the change rates of anti-PEG antibody) as fixed effect and subject as random effect were considered in LMM.

In addition, ▲Anti-PEG IgM (Log_{10} CONC) was defined as Anti-PEG IgM (Log_{10} $CONC_{2nd\ injection}$) ($\log_{10}$-transformed concentration of anti-PEG IgM induced during the second injection cycle) subtracting corresponding Anti-PEG IgM (Log_{10} $CONC_{1st\ injection}$) ($\log_{10}$-transformed concentrations of anti-PEG IgM induced during the first injection cycle). Similarly, ▲Anti-PEG IgG (Log_{10} CONC) was calculated by subtracting Anti-PEG IgG (Log_{10} $CONC_{1st\ injection}$) ($\log_{10}$-transformed concentrations of anti-PEG IgG

456 induced during the first injection cycle) from the corresponding Anti-PEG IgG (Log_{10} $CONC_{2nd\ injection}$)
457 (log_{10}-transformed concentration of anti-PEG IgG induced during the second injection cycle). Differences
458 in ▲Anti-PEG IgM (Log_{10} CONC) or ▲Anti-PEG IgG (Log_{10} CONC) among various groups at each time
459 point were analyzed with Mann-Whitney U test using R 4.0.5, with *P* values adjusted for FDR (false
460 discovery rate). Changing curves of average level of ▲Anti-PEG IgM (Log_{10} CONC) or ▲Anti-PEG IgG
461 (Log_{10} CONC) over time for various doses were fitted by the R package called "ggalt". Profile analysis was
462 performed to examine whether the overall trends of changing curves of average level of ▲Anti-PEG IgM
463 (Log_{10} CONC) or ▲Anti-PEG IgG (Log_{10} CONC) over time between every two groups were equal. The
464 analysis included two parts: parallel test and coincidence test. Only when the two changing curves of average
465 level of ▲Anti-PEG IgM (Log_{10} CONC) or ▲Anti-PEG IgG (Log_{10} CONC) met both parallel and
466 coincidence test, the overall trend of the two changing curves of average level of ▲Anti-PEG IgM (Log_{10}
467 CONC) or ▲Anti-PEG IgG (Log_{10} CONC) was considered as no difference. According to factorial design
468 (group × time) and repeated measures of antibody level, LMM were conducted to compare the change rates
469 and average levels of ▲Anti-PEG IgM (Log_{10} CONC) or ▲Anti-PEG IgG (Log_{10} CONC) across groups,
470 with all time points included. Several variables, including group (indicating mean differences in the average
471 levels of ▲Anti-PEG IgM (Log_{10} CONC) or ▲Anti-PEG IgG (Log_{10} CONC)), time, $time^2$, and interaction
472 term of group and time (indicating mean differences in the change rates of ▲Anti-PEG IgM (Log_{10} CONC)
473 or ▲Anti-PEG IgG (Log_{10} CONC) levels) as fixed effect and subject as random effect were considered in
474 LMM. After performing the Shapiro-Wilk test to check for normality and the F test to check for variance
475 homogeneity, data obtained in the biodistribution and blood clearance study were analyzed using multiple
476 unpaired *t* tests with correction for multiple comparisons using Prism 9.2.0 (GraphPad Software, San Diego,
477 USA). $P < 0.05$ was considered statistically significant.
478

479 **Data availability**

480 All data supporting the findings of this study are available within the paper and Supplementary

Information. The associated raw data are available from the corresponding author on reasonable request.

Acknowledgments

The authors would like to gratefully acknowledge Shenghai Chang and Lingyun Wu in the Center of Cryo-Electron Microscopy (CCEM), Zhejiang University for their technical assistance on Cryo-EM. The authors would like to gratefully acknowledge Yanhong Chen in the Laboratory Animal Center, Zhejiang University for her technical assistance on animal experiments. The authors acknowledge support from the National Natural Science Foundation of China (21722405 and 22075243 to Dr. Meihua Sui), Zhejiang Provincial Natural Science Foundation of China (LZ23E030003 to Dr. Meihua Sui) and Startup Foundation for Hundred-Talent Program of Zhejiang University (to Dr. Meihua Sui).

Competing interests

The authors declare that there are no competing interests.

Author contributions

M.S., the principal investigator of the major supporting grants, and H.W. conceived the research project and defined the goals of the present study. M.S., H.W. and Y.W. designed the experiments. H.W. and Y.W. performed most experiments. M.S., H.W., Y.W., C.Y., X.X. and Y.H. discussed this project and analyzed the data. X.X. provided technical/platform supports. W.Z., H.L., Y.Z., G.L. and J.S. helped with the animal experiments. H.W., Y.W., C.Y. and Y.H. drafted the manuscript. M.S., H.W., Y.W., C.Y. and Y.H. revise and edited the manuscript. These authors contributed equally: H.W., Y.W. and C.Y.

References

1. Mendes, B.B. *et al.* Nanodelivery of nucleic acids. *Nat. Rev. Methods Primers* **2**, 24 (2022).

2. Curreri, A., Sankholkar, D., Mitragotri, S. & Zhao, Z. RNA therapeutics in the clinic. *Bioeng. Transl. Med.* e10374 (2022).

3. Suk, J.S., Xu, Q.G., Kim, N., Hanes, J. & Ensign, L.M. PEGylation as a strategy for improving nanoparticle-based drug and gene delivery. *Adv. Drug Deliver. Rev.* **99**, 28-51 (2016).

506 4. Khurana, A. *et al.* Role of nanotechnology behind the success of mRNA vaccines for COVID-19. *Nano*
507 *Today* **38**, 101142 (2021).
508 5. Chen, B.M., Cheng, T.L. & Roffler, S.R. Polyethylene glycol immunogenicity: theoretical, clinical, and
509 practical aspects of anti-polyethylene glycol antibodies. *ACS Nano* **15**, 14022-14048 (2021).
510 6. Ibrahim, M. *et al.* Polyethylene glycol (PEG): the nature, immunogenicity, and role in the hypersensitivity
511 of PEGylated products. *J. Control. Release* **351**, 215-230 (2022).
512 7. Yang, Q. & Lai, S.K. Anti-PEG immunity: emergence, characteristics, and unaddressed questions. *Wiley*
513 *Interdiscip. Rev. Nanomed. Nanobiotechnol.* **7**, 655-677 (2015).
514 8. Shi, D. *et al.* To PEGylate or not to PEGylate: immunological properties of nanomedicine's most popular
515 component, polyethylene glycol and its alternatives. *Adv. Drug Deliver. Rev.* **180**, 114079 (2022).
516 9. Chen, B.M. *et al.* Measurement of pre-existing IgG and IgM antibodies against polyethylene glycol in
517 healthy individuals. *Anal. Chem.* **88**, 10661-10666 (2016).
518 10. Yang, Q. *et al.* Analysis of pre-existing IgG and IgM antibodies against polyethylene glycol (PEG) in the
519 general population. *Anal. Chem.* **88**, 11804-11812 (2016).
520 11. Ju, Y. *et al.* Impact of anti-PEG antibodies induced by SARS-CoV-2 mRNA vaccines. *Nat. Rev. Immunol.*
521 **23**, 1-2 (2022).
522 12. Zhang, X.P. *et al.* Patisiran pharmacokinetics, pharmacodynamics, and exposure-response analyses in
523 the phase 3 APOLLO trial in patients with hereditary transthyretin-mediated (hATTR) amyloidosis. *J. Clin.*
524 *Pharmacol.* **60**, 37-49 (2020).
525 13. Ju, Y. *et al.* Anti-PEG antibodies boosted in humans by SARS-CoV-2 lipid nanoparticle mRNA vaccine.
526 *ACS Nano* **16**, 11769-11780 (2022).
527 14. Guerrini, G. *et al.* Monitoring anti-PEG antibodies level upon repeated lipid nanoparticle-based COVID-
528 19 vaccine administration. *Int. J. Mol. Sci.* **23**, 8838 (2022).
529 15. Carreño, J.M. *et al.* mRNA-1273 but not BNT162b2 induces antibodies against polyethylene glycol
530 (PEG) contained in mRNA-based vaccine formulations. *Vaccine* **40**, 6114-6124 (2022).

531 16. Bavli, Y. *et al*. Anti-PEG antibodies before and after a first dose of Comirnaty (mRNA-LNP-based
532 SARS-CoV-2 vaccine). *J. Control. Release* **354**, 316-322 (2023).
533 17. ONPATTRO-Prescribing Information, https://www.alnylam.com/sites/default/files/pdfs/ONPATTRO-
534 Prescribing-Information.pdf (2023).
535 18. Food and Drug Administration. Comirnaty Information-Summary basis for regulatory action, 8
536 November, 2021; https://www.fda.gov/media/151733/download
537 19. Food and Drug Administration. Spikevax Information-Summary basis for regulatory action, 30 January,
538 2022; https://www.fda.gov/media/155931/download
539 20. World Health Organization. WHO guidelines on non-clinical evaluation of vaccines, WHO Technical
540 Report Series No. 927, Annex 1, 1 January 2005; https://cdn.who.int/media/docs/default-
541 source/biologicals/vaccine-standardization/annex-1nonclinical.p31-
542 63.pdf?sfvrsn=e87c28d8_3&download=true
543 21. Yang, K., Reker-Smit, C., Stuart, M.C.A. & Salvati, A. Effects of protein source on liposome uptake by
544 cells: corona composition and impact of the excess free proteins. *Adv. Healthc. Mater.* **10**, e2100370 (2021).
545 22. Naumenko, V.A. *et al.* Intravital imaging of liposome behavior upon repeated administration: a step
546 towards the development of liposomal companion diagnostic for cancer nanotherapy. *J. Control. Release*
547 **330**, 244-256 (2021).
548 23. Food and Drug Administration. Guidance for industry: bioanalytical method validation.
549 http://www.fda.gov/downloads/Drugs/GuidanceComplianceRegulatoryInformation/Guidances/ucm070107
550 .pdf. (2018)
551 24. Findlay, J.W.A. *et al.* Validation of immunoassays for bioanalysis: a pharmaceutical industry perspective.
552 *J. Pharmaceut. Biomed.* **21**, 1249-1273 (2000).
553 25. European Medicines Agency. Spikevax (previously COVID-19 Vaccine Moderna) : EPAR - Public
554 assessment report, 20 January 2021; https://www.ema.europa.eu/en/documents/assessment-report/spikevax-
555 previously-covid-19-vaccine-moderna-epar-public-assessment-report_en.pdf

556 26. European Medicines Agency. Comirnaty : EPAR - Public assessment report, 23 December 2020;
557 https://www.ema.europa.eu/en/documents/assessment-report/comirnaty-epar-public-assessment-
558 report_en.pdf
559 27. Defrance, T., Taillardet, M. & Genestier, L. T cell-independent B cell memory. *Curr. Opin. Immunol.* **23**,
560 330-336 (2011).
561 28. Ichihara, M. *et al.* Anti-PEG IgM response against PEGylated liposomes in mice and rats. *Pharmaceutics*
562 **3**, 1-11 (2010).
563 29. Zhang, N.N. *et al.* A thermostable mRNA vaccine against COVID-19. *Cell* **182**, 1271-1283 (2020).
564 30. Stewart, J.C.M. Colorimetric determination of phospholipids with ammonium ferrothiocyanate. *Anal.*
565 *Biochem.* **104**, 10-14 (1980).
566 31. Nair, A., Morsy, M.A. & Jacob, S. Dose translation between laboratory animals and human in preclinical
567 and clinical phases of drug development. *Drug Develop. Res.* **79**, 373-382 (2018).
568 32. American Veterinary Medical Association. AVMA guidelines for the euthanasia of animals: 2020 Edition,
569 24 February 2020; https://www.avma.org/sites/default/files/2020-02/Guidelines-on-Euthanasia-2020.pdf
570 33. Draper, N. R., & Smith, H. Applied regression analysis (3rd ed.) (Wiley Press, New York, 1998).
571

572 **Figures**

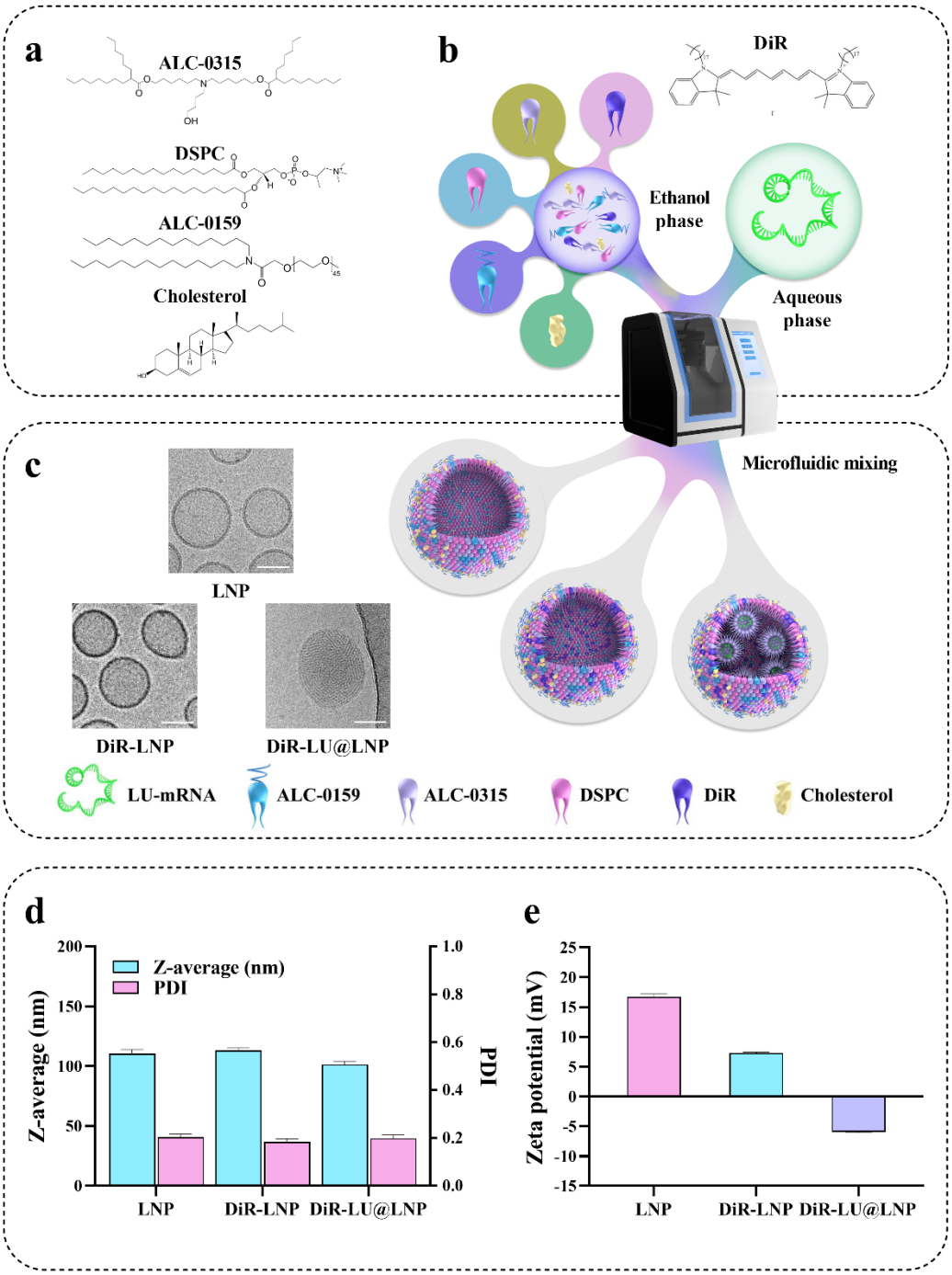

573

574 **Fig. 1. Preparation and characterization of LNP, DiR-LNP and DiR-LU@LNP.** (**a**) Chemical structures
575 of lipid compositions in LNP carrier of COVID-19 vaccine Comirnaty®. (**b**) Schematic illustration of the
576 synthesis of LNP, DiR-LNP and DiR-LU@LNP. Briefly, the ethanol phase was combined with the aqueous
577 phase at a flow rate ratio of 1: 3 (ethanol: aqueous) through a microfluidic mixing device. (**c**) Representative

578 cryogenic transmission electron microscopy (Cryo-TEM) images of LNP, DiR-LNP and DiR-LU@LNP.
579 Scale bar: 50 nm. (**d**) Hydrodynamic size (Z-average) and polydispersity index (PDI) of LNP, DiR-LNP and
580 DiR-LU@LNP measured by DLS. (**e**) Zeta potential of LNP, DiR-LNP and DiR-LU@LNP measured by
581 DLS. Data in **d** and **e** were presented as "mean ± standard deviation" (n=3). LNP, lipid nanoparticles; DLS,
582 dynamic light scattering; LU-mRNA: luciferase mRNA.
583

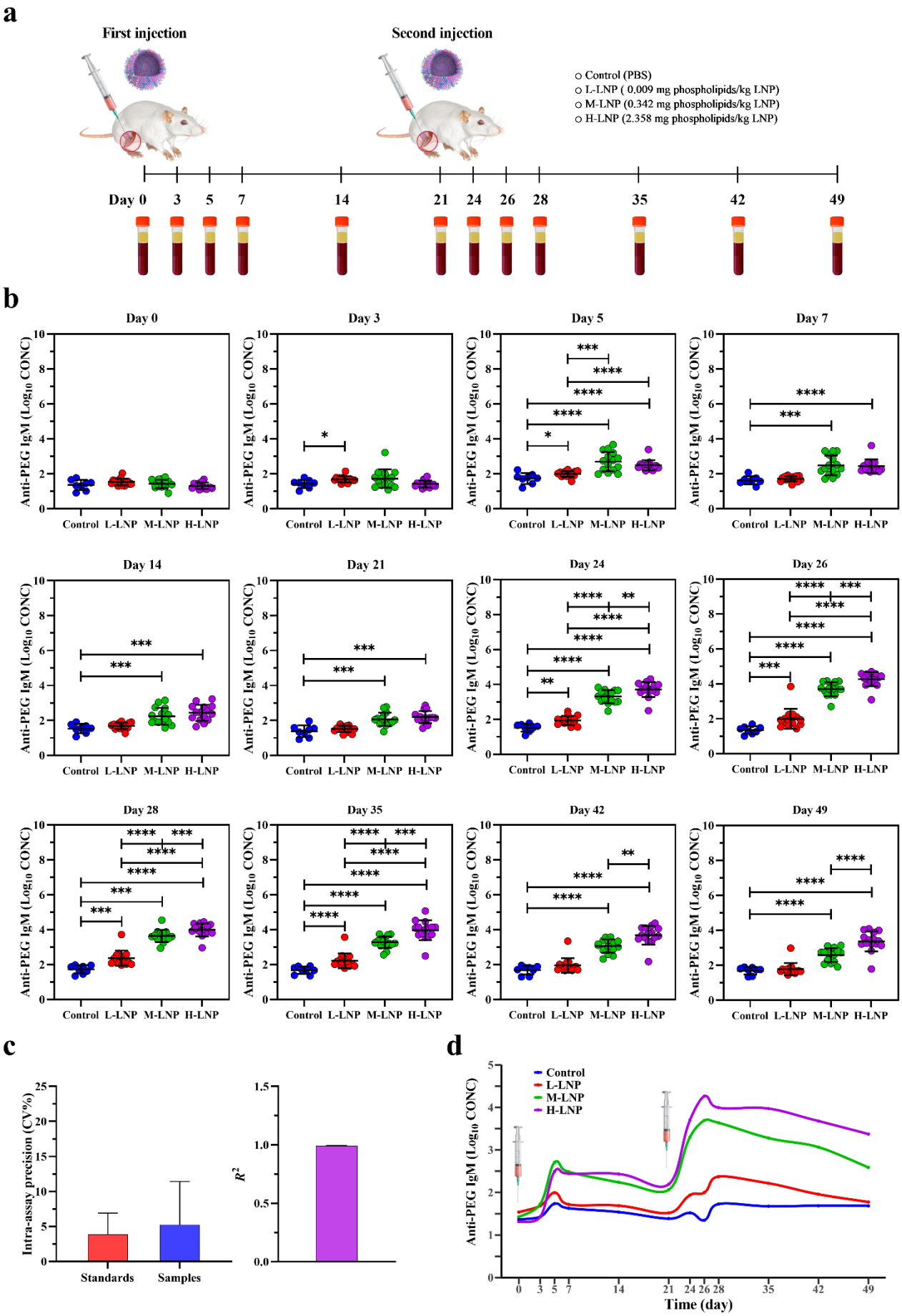
a
First injection
Second injection
Control (PBS)
L-LNP (0.009 mg phospholipids/kg LNP)
M-LNP (0.342 mg phospholipids/kg LNP)
H-LNP (2.358 mg phospholipids/kg LNP)
Day 0
3
5
7
14
21
24
26
28
35
42
49
b
Day 0
Day 3
Day 5
Day 7
Day 14
Day 21
Day 24
Day 26
Day 28
Day 35
Day 42
Day 49
Anti-PEG IgM (Log10 CONC)
Control
L-LNP
M-LNP
H-LNP
c
Intra-assay precision (CV%)
Standards
Samples
R2
d
Control
L-LNP
M-LNP
H-LNP
Anti-PEG IgM (Log10 CONC)
Time (day)

584

585 **Fig. 2. Experimental design and evaluation of anti-PEG IgM production in rat.** (**a**) Schematic
586 illustration of the experimental protocols. Wistar rats were injected intramuscularly with 0.009 (L-LNP
587 group), 0.342 (M-LNP group) or 2.358 (H-LNP group) mg phospholipids/kg LNP on Day 0 and Day 21,
588 respectively. Rats in the Control group were injected with PBS. Serum samples were collected at the
589 indicated time points (Day 0, 3, 5, 7, 14, 21, 24, 26, 28, 35, 42 and 49) for further evaluation of the presence
590 and level of anti-PEG antibodies with ELISA. (**b**) Quantitative analysis of anti-PEG IgM (Log_{10} CONC)
591 (log_{10}-transformed concentration of anti-PEG IgM) induced by LNP in rat serum. Data were presented as
592 "mean ± standard deviation", with n = 8 for Control group and n = 15 for all LNP-treated groups. Differences
593 in anti-PEG IgM (Log_{10} CONC) among various groups were analyzed using Mann-Whitney U test, with *P*
594 values adjusted for FDR (false discovery rate). Peak levels of anti-PEG IgM (Log_{10} CONC) induced during
595 the initial and second injection cycle were as follows: L-LNP, 1.996 on Day 5 and 2.374 on Day 28; M-LNP,
596 2.704 on Day 5 and 3.692 on Day 26; H-LNP, 2.492 on Day 5 and 4.262 on Day 26. *, $P < 0.05$; **, $P <$
597 0.01; ***, $P < 0.001$; ****, $P < 0.0001$. (**c**) Representative quality control data of ELISA for detecting anti-
598 PEG IgM. The left image shows the intra-assay precision/Coefficient of Variation (CV%) of anti-PEG IgM
599 standards (CV% = 3.884 ± 3.046%) and serum samples (CV% = 5.237 ± 6.192%), and the right image shows
600 the goodness of fit/coefficient of determination ($R^2 = 0.992 \pm 0.004$) of the standard curve (see **Methods** for
601 acceptance criteria). Data were presented as "mean ± standard deviation", with n = 56 for intra-assay
602 precision (CV%) of anti-PEG IgM standards, n = 636 for intra-assay precision (CV%) of serum samples and
603 n = 8 for R^2. (**d**) Time-course of anti-PEG IgM induced by PEGylated LNP. The changing curves of mean
604 anti-PEG IgM (Log_{10} CONC) levels over time were fitted by the R package called "ggalt".
605

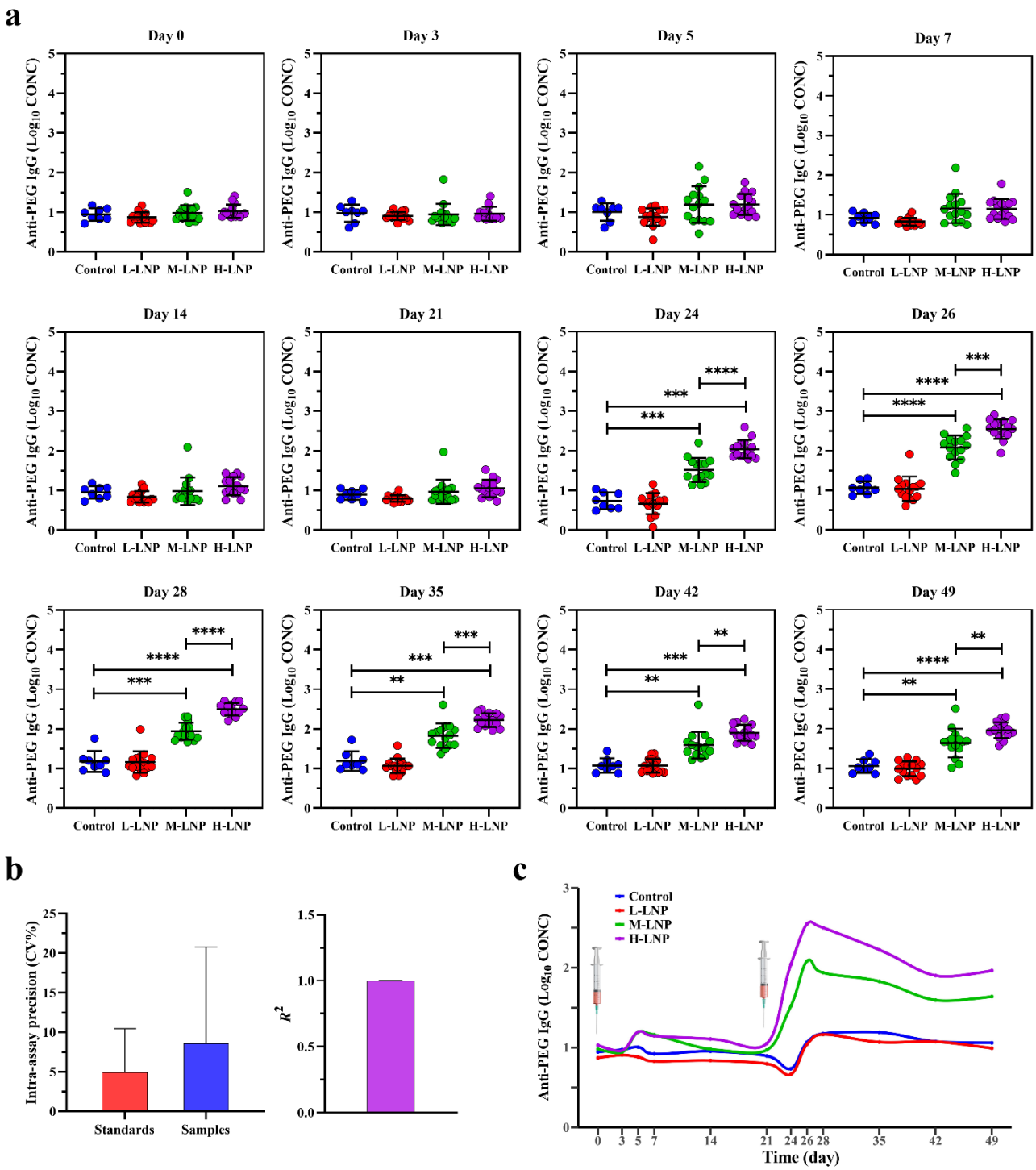

Fig. 3. Evaluation of anti-PEG IgG production in rat. (**a**) Quantitative analysis of anti-PEG IgG (Log_{10} CONC) (log_{10}-transformed concentration of anti-PEG IgG) induced by LNP in rat serum. Data were presented as "mean ± standard deviation", with n = 8 for Control group and n = 15 for all LNP-treated groups. Differences in anti-PEG IgG (Log_{10} CONC) among various groups were analyzed using Mann-Whitney U test, with *P* values adjusted for FDR (false discovery rate). Peak levels of anti-PEG IgG (Log_{10} CONC)

612 induced during the second injection cycle were as follows: M-LNP, 2.083 on Day 26; H-LNP, 2.547 on Day
613 26. *, $P < 0.05$; **, $P < 0.01$; ***, $P < 0.001$; ****, $P < 0.0001$. (**b**) Representative quality control data of
614 ELISA for detecting anti-PEG IgG. The left image shows the intra-assay precision/Coefficient of Variation
615 (CV%) of anti-PEG IgG standards (CV% = 4.897 ± 5.549%) and serum samples (CV% = 8.546 ± 12.211%),
616 and the right image shows the goodness of fit/coefficient of determination (R^2 = 0.999 ± 0.001) of the
617 standard curve (see **Methods** for acceptance criteria). Data were presented as "mean ± standard deviation",
618 with n = 56 for intra-assay precision (CV%) of anti-PEG IgM standards, n = 636 for intra-assay precision
619 (CV%) of serum samples and n = 8 for R^2. (**c**) Time-course of anti-PEG IgG induced by PEGylated LNP.
620 The changing curves of mean anti-PEG IgG (Log_{10} CONC) levels over time were fitted by the R package
621 called "ggalt".
622

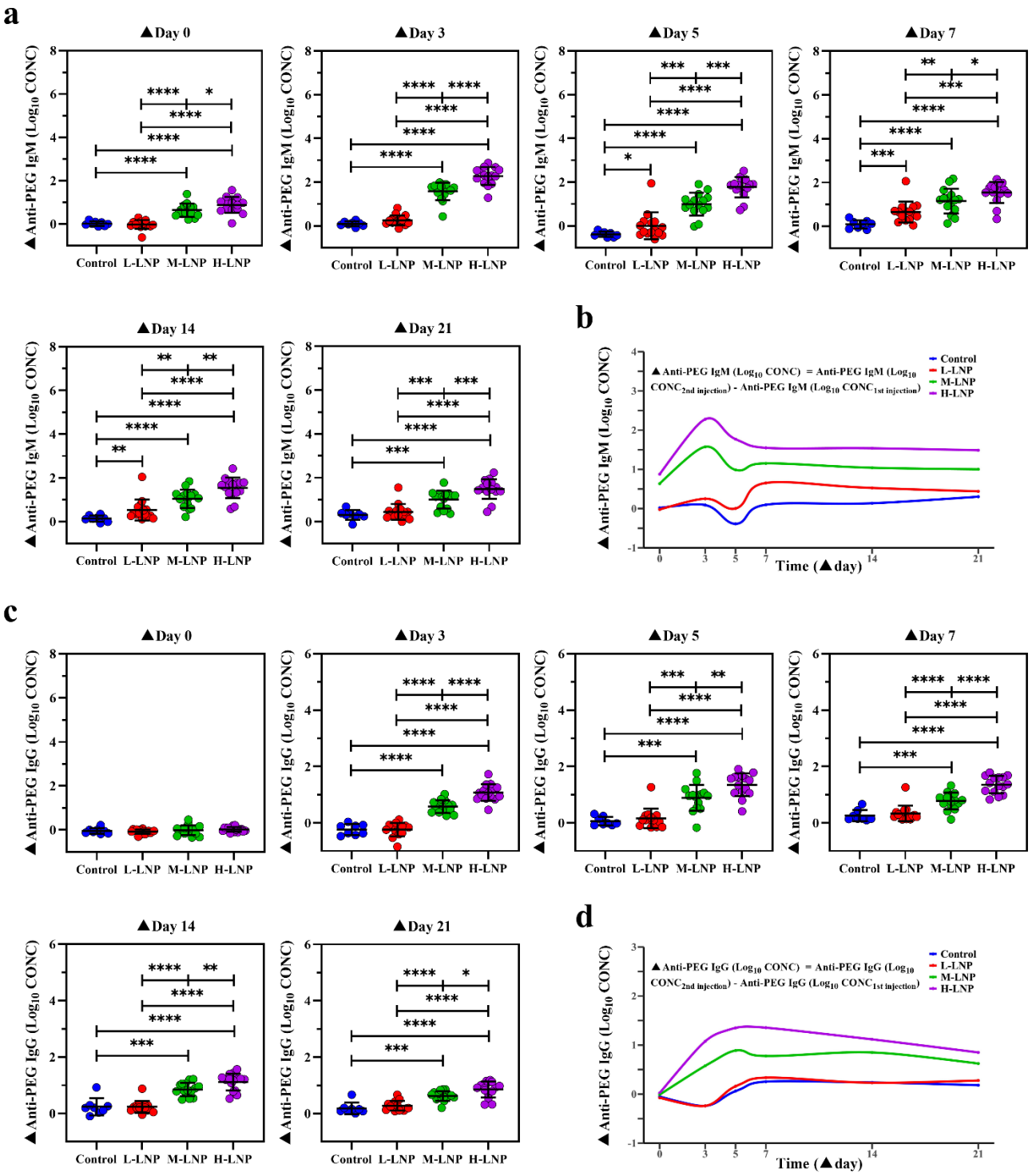

Fig. 4. Enhanced production of anti-PEG antibodies in rat by repeated administration with PEGylated LNP. (**a**) Enhanced anti-PEG IgM production induced by repeated LNP injection. ▲Anti-PEG IgM (Log_{10} CONC) means Anti-PEG IgM (Log_{10} $CONC_{2nd\ injection}$) (log_{10}-transformed concentration of anti-PEG IgM induced during the second injection cycle) subtracted corresponding Anti-PEG IgM (Log_{10} $CONC_{1st\ injection}$)

628 (log_{10}-transformed concentrations of anti-PEG IgM induced during the first injection cycle). Peak levels of
629 ▲Anti-PEG IgM (Log_{10} CONC) induced by different LNP doses were 0.654 ± 0.471 for L-LNP (▲Day 7),
630 1.574 ± 0.399 for M-LNP (▲Day 3) and 2.277 ± 0.410 for H-LNP (Day 3), respectively, with significant
631 difference among three groups ($P < 0.001$ for M-LNP *vs* L-LNP; $P < 0.0001$ for H-LNP vs L-LNP; $P<0.0001$
632 for H-LNP *vs* M-LNP). (**b**) Time-course of enhanced anti-PEG IgM induced by repeated injection of LNP.
633 (**c**) Enhanced anti-PEG IgG production induced by repeated injection of LNP. ▲Anti-PEG IgG (Log_{10}
634 CONC) means Anti-PEG IgG (Log_{10} $CONC_{2nd\ injection}$) (log10-transformed concentration of anti-PEG IgG
635 induced during the second injection cycle) subtracted corresponding Anti-PEG IgG (Log_{10} $CONC_{1st\ injection}$)
636 (log_{10}-transformed concentrations of anti-PEG IgG induced during the first injection cycle). Peak levels of
637 ▲Anti-PEG IgG (Log_{10} CONC) induced by different LNP doses were 0.888 ± 0.459 for M-LNP (▲Day 5)
638 and 1.354 ± 0.308 for H-LNP (▲Day 7), respectively, with significant difference between these two groups
639 ($P < 0.01$). (**d**) Time-course of enhanced anti-PEG IgG induced by repeated injection of LNP. In figure **a** and
640 **c**, data were presented as "mean ± standard deviation", with n = 8 for Control group and n = 15 for all LNP-
641 treated groups. Differences in ▲Anti-PEG IgM (Log_{10} CONC) or ▲Anti-PEG IgG (Log_{10} CONC) among
642 various groups were analyzed using Mann-Whitney U test, with *P* values adjusted for FDR (false discovery
643 rate). *, $P < 0.05$; **, $P < 0.01$; ***, $P < 0.001$; ****, $P < 0.0001$. In Figure **b** and **d**, changing curves of
644 average level of ▲Anti-PEG IgM (Log_{10} CONC) or ▲Anti-PEG IgG (Log_{10} CONC) over time for various
645 doses were fitted by the R package called "ggalt".
646

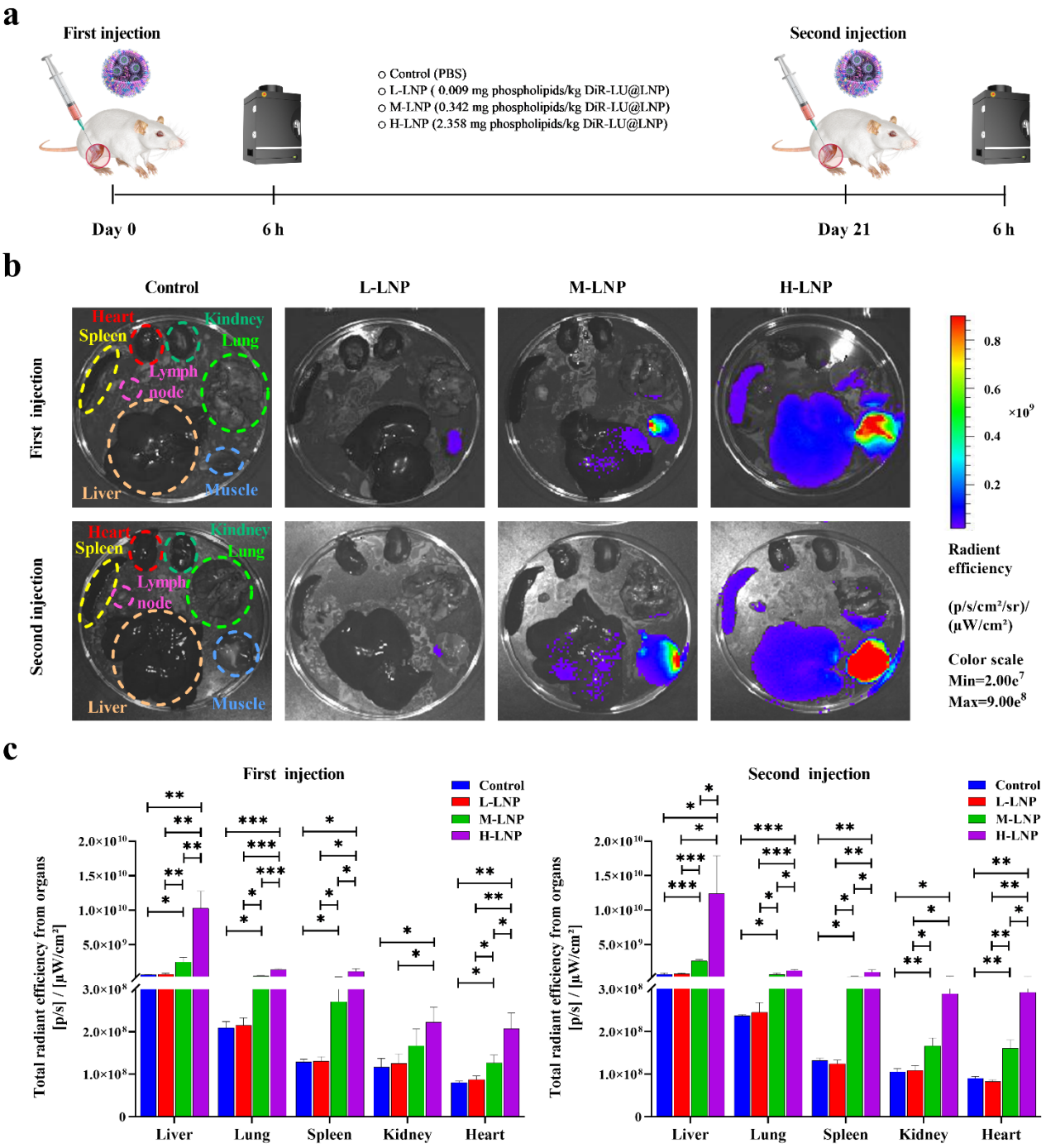

Fig. 5. Experimental design and biodistribution of PEGylated LNP in representative organs of rat. (**a**) Schematic illustration of the experimental protocols. Wistar rats were injected intramuscularly with 0.009 (L-LNP group), 0.342 (M-LNP group) or 2.358 (H-LNP group) mg phospholipids/kg DiR-LU@LNP on Day 0 and Day 21, respectively. Rats in the Control group were injected with PBS. Six hours after each injection, three rats from each experimental group were sacrificed and immediately dissected. Major organs including heart, liver, spleen, lung, kidneys and draining lymph node, and muscle at the injection site were collected

654 for fluorescence imaging with IVIS Spectrum imaging system. (**b**) Representative fluorescence images of
655 major organs and muscle tissues isolated from rats 6 hours after the first and second injection of DiR-
656 LU@LNP. (**c**) Total radiant efficiency of major organs determined 6 hours after the first and second injection
657 of DiR-LU@LNP. Data were presented as "mean ± standard deviation" (n = 3). Differences in total radiation
658 efficiency induced by three doses were analyzed using multiple unpaired *t* tests with correction for multiple
659 testing. *, $P < 0.05$; **, $P < 0.01$; ***, $P < 0.001$; ****, $P < 0.0001$.
660

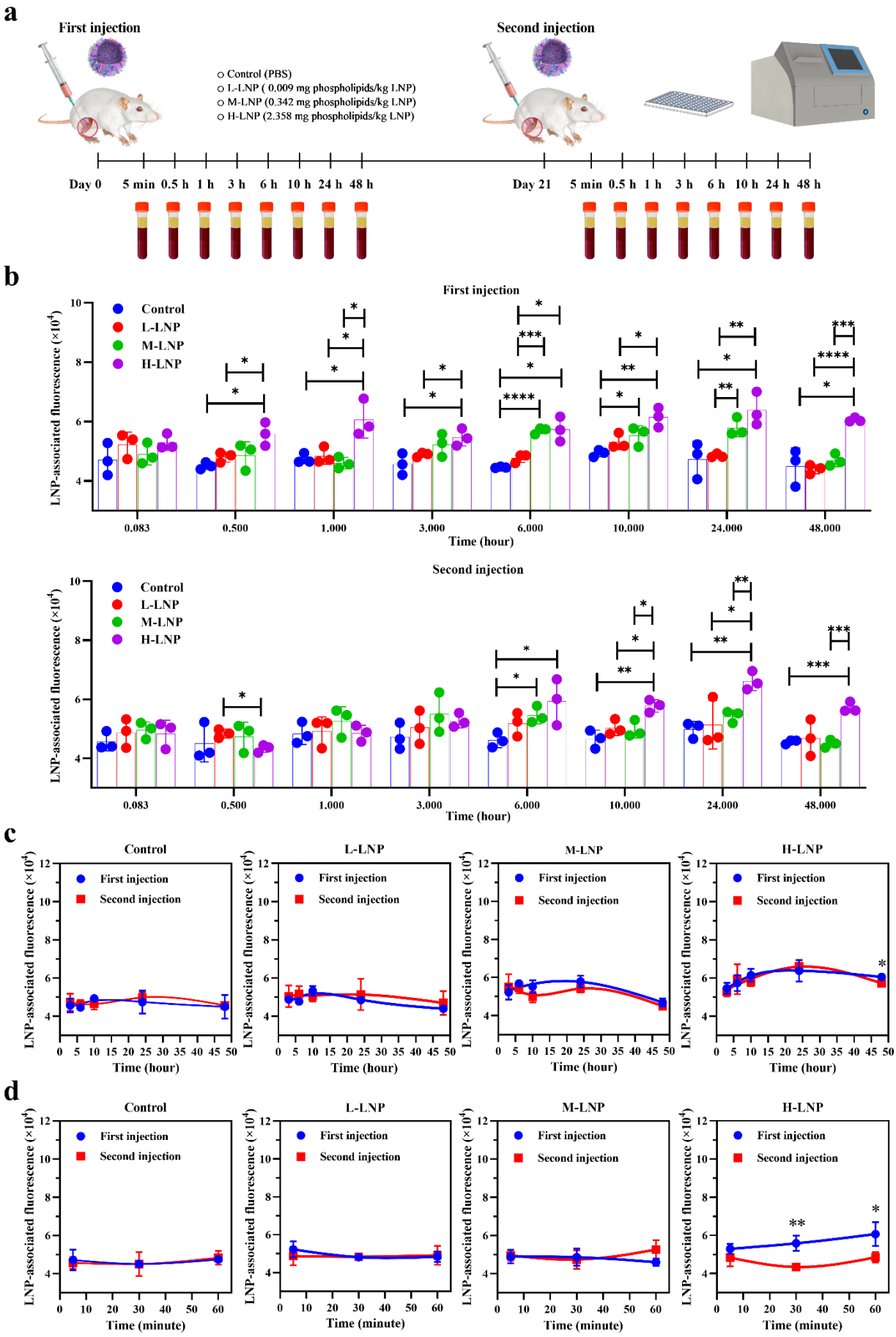
a
First injection
Second injection
Control (PBS)
L-LNP (0.009 mg phospholipids/kg LNP)
M-LNP (0.342 mg phospholipids/kg LNP)
H-LNP (2.358 mg phospholipids/kg LNP)
Day 0
5 min
0.5 h
1 h
3 h
6 h
10 h
24 h
48 h
Day 21
b
First injection
Second injection
Control
L-LNP
M-LNP
H-LNP
LNP-associated fluorescence (×10^4)
Time (hour)
0.083
0.500
1.000
3.000
6.000
10.000
24.000
48.000
c
Control
L-LNP
M-LNP
H-LNP
First injection
Second injection
LNP-associated fluorescence (×10^4)
Time (hour)
d
Control
L-LNP
M-LNP
H-LNP
First injection
Second injection
LNP-associated fluorescence (×10^4)
Time (minute)

662 **Fig. 6. Experimental design and blood clearance of PEGylated LNP in rats.** (**a**) Schematic illustration
663 of the experimental protocols. Wistar rats were injected intramuscularly with 0.009 (L-LNP group), 0.342
664 (M-LNP group) or 2.358 (H-LNP group) mg phospholipids/kg DiR-LNP on Day 0 and Day 21, respectively.
665 Rats in the Control group were injected with PBS. Serum samples were collected at the indicated 8 time
666 points (5 minutes, 30 minutes, 1 hour, 3 hours, 6 hours, 10 hours, 24 and 48 hours) after each injection of
667 DiR-LNP, followed by determination of LNP-associated fluorescence with Spectramax ID5 fluorescent
668 spectrometry. (**b**) LNP-associated fluorescence was presented as "mean ± standard deviation" (n = 3) for
669 each group, with differences among various groups after each injection analyzed using the multiple unpaired
670 *t* test, with *P* values adjusted for FDR (false discovery rate). *, $P < 0.05$; **, $P < 0.01$; ***, $P < 0.001$; ****,
671 $P < 0.0001$. (**c**) Blood clearance profile of DiR-LNP in rats based on LNP-associated fluorescence obtained
672 at 3 hours, 6 hours, 10 hours, 24 and 48 hours, with fitted curves created by Prism 9.2.0 (GraphPad Software).
673 (**d**) Blood clearance profile of DiR-LNP in rats based on LNP-associated fluorescence obtained at 5 minutes,
674 30 minutes and 1 hour, with fitted curves created by Prism 9.2.0 (GraphPad Software). As the earliest three
675 time points presented in **d** would become invisible if combined with 5 later time points, blood clearance
676 profile of DiR-LNP based on all 8 time points was presented as two parts (**c** and **d**). Data in **c** and **d** were
677 presented as "mean ± standard deviation" (n = 3) for each group, with differences between two injections
678 analyzed using the multiple unpaired *t* test, with *P* values adjusted for FDR (false discovery rate). *, $P <$
679 0.05; **, $P < 0.01$; ***, $P < 0.001$; ****, $P < 0.0001$.